

From: DEFORMATION OF CERAMIC MATERIALS II
Edited by Richard E. Tressler and Richard C. Bradt
(Plenum Publishing Corporation, 1984)

DEFORMATION-INDUCED CRACK INITIATION BY INDENTATION OF SILICATE
MATERIALS

H. Multhopp, B.R. Lawn and T.P. Dabbs

Center for Materials Science
National Bureau of Standards
Washington, DC 20234

ABSTRACT

The micromechanics of radial crack initiation produced in indentation of soda-lime glass, fused silica and quartz are discussed in terms of a two-step, nucleation and growth model. Particular attention is focussed on the strong rate effects in the presence of environmental water, as manifested by a tendency to delayed crack pop in with decreasing contact duration. Microscopic examination of the indentations indicates that deformation "shear faults", which accommodate the intense strains associated with the penetrating indenter, control the kinetics of the initiation process. The geometrical constraints which determine the stress concentrations for crack nucleation from these faults are structure-sensitive.

INTRODUCTION

Recent studies on the micromechanical response of soda-lime glass in Vickers indentation have shed new light on the mechanisms of crack initiation in brittle amorphous solids.¹⁻³ Essentially, the initiation process takes place within the deformation zone beneath the indenter, and thereby generates characteristic "radial" cracks from the corners of the impression.^{4,5} There is an intrinsic scale effect in this process, in that the radial cracks appear only above some threshold in the loading; fracture instability may be identified with the attainment of a critical flaw size in the near-contact region.^{6,7} The feature of this threshold which is arousing the greatest current interest, particularly in the context of strength in the ultra-small flaw region (e.g. optical fibers),^{8,9} is a strong rate dependence in

the presence of environmental moisture.¹ The rate effect is most dramatically manifested as an increasing tendency for the radial cracks to "pop in" after completion of the indentation cycle with decreasing height or width of the force-time pulse. Attempts to model the kinetic response have thus far been restricted to qualitative descriptions of the nucleation and growth of microcracks from incipient "shear faults" within the deformation zone, with due recognition of the residual contact field as a primary driving force.¹

In this paper we expand our data base on soda-lime glass, and extend our material compass to two other silicate modifications, fused silica and quartz. Fused silica is known to be "anomalous" in its deformation behavior, in that the penetrating indenter is accommodated by a densification rather than by a cooperative shear failure of the glass structure.¹⁰ Quartz, the "ordered" counterpart of fused silica, introduces a crystallographic element into the indentation response. By encompassing a broader range of deformation modes we may hope to gain some insight into the fundamental structural requirements for the operation of crack initiation processes, and ultimately to develop quantitative models for characterizing flaws in the subthreshold region.

EXPERIMENTAL

A schematic of the experimental arrangement used to observe the indentations is shown in Fig. 1. The Vickers indenter arm is activated by an electromagnetic coil drive, with facility to control (via a function generator) the load-time pulse, $P(t)$. A piezoelectric cell in the arm allows for continuous monitoring of this pulse. The most commonly used pulse shapes in our experiments are square and half-sine, characterized by height P_m and base-width T . The indenter system seats on to the stage of an inverted microscope for in situ viewing of the contact area. In this way the pop-in time t_c from start of the pulse to appearance of the first radial crack can be measured directly. The specimen is housed within a simple enclosure for environmental control.

The soda-lime and fused silica glass specimens were in the form of microscope slides. Quartz specimens were cut from synthetic single crystals, parallel to the basal plane. Some of the specimens were specially prepared for post-indentation examination by scanning electron microscopy for clues as to the nature of the underlying initiation processes.

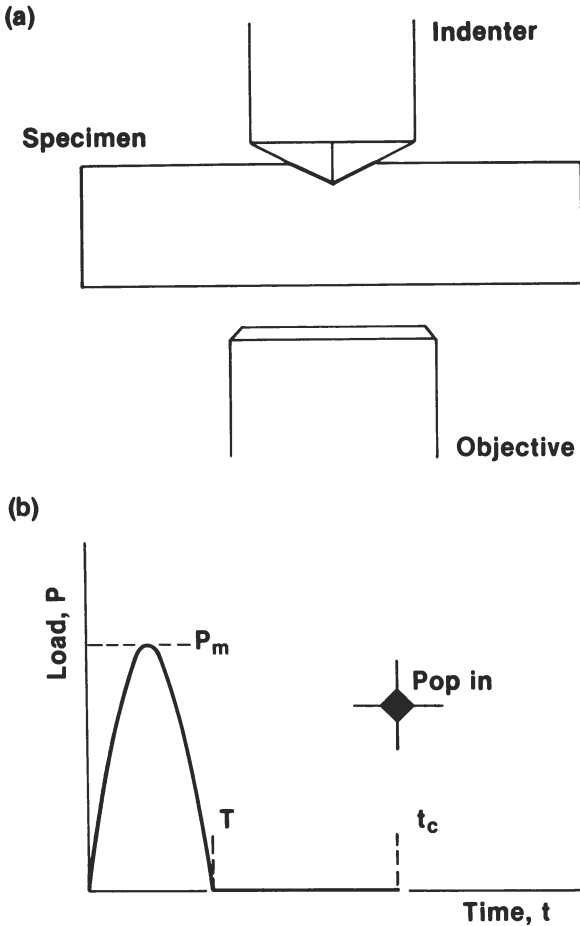


Figure 1. (a) Schematic of optical system for in situ viewing of Vickers indentations in transparent specimens. (b) Definition of load-time parameters used to characterize kinetics of radial crack pop in.

RESULTS

Radial Pop-in Kinetics

Let us now examine some of the more general features of the delayed pop-in kinetics. Figure 2 illustrates the influence of environment and indentation load on the fracture time response.

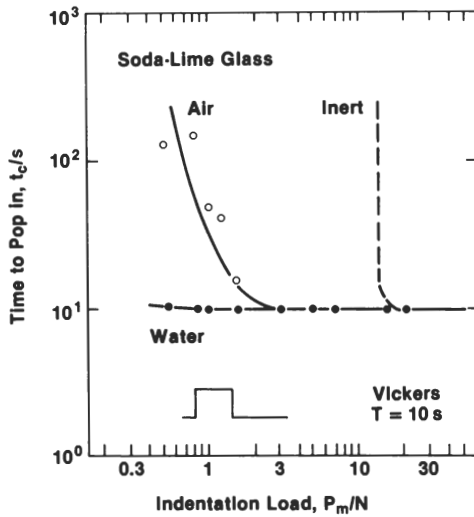


Figure 2. Median times to radial crack pop in as function of square pulse peak load, at fixed contact duration, for soda-lime glass in different environments.

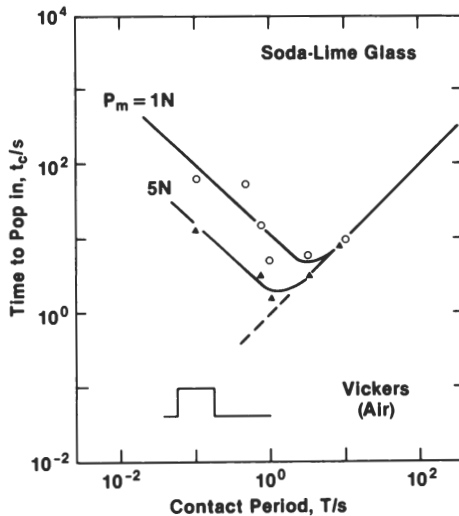


Figure 3. Median times to radial crack pop in as function of square pulse indentation hold time, at fixed peak loads, for soda-lime glass in air.

The data in this figure are for soda-lime glass using square-shaped load pulses of fixed duration 10 s. For the inert environment (dry N_2 gas) there is a well-defined cutoff load below which radial cracks cannot be made to pop in. In water, on the other hand, pop in occurs almost spontaneously as the indenter is removed, down toward the lowest attainable loads with our apparatus. An intermediate response is observed in air (55% relative humidity). Thus the delay time for radial cracking increases as the indentation load and the moisture content in the environment diminish.

The influence of contact duration is seen in Fig. 3. These data are for loads of 1 N and 5 N on soda-lime glass in air, taken under effectively the same test conditions as represented in Fig. 2. The delays to pop in increase abruptly below some critical duration, or "incubation time", this quantity diminishing with increasing load.

The use of square load pulses to obtain the data in Figs. 2 and 3 immediately provides us with useful information as to the nature of the critical condition for pop in. The fact that even under the most conducive of fracture conditions (i.e. high water contents, large loads, or long contact times) initiation occurs only on unloading the indenter means that some constraint must exist to prevent radial development while the system is maintained at maximum load. (Actually, at sufficiently high loads, well above the threshold limits defined here, cracks can generate on loading, but these are of a different kind - subsurface medians rather than surface radials.¹) On the other hand, it is impossible with square pulses to determine exactly where on unloading this constraint is released.

It is in this context that the facility to change over to half-sine pulses proved useful. With this continuous load-time function it could be established that the constraint on crack instability disappears at $P \approx 0.3 P_m$, on the unload half-cycle, marking the instant at which the residual field begins to dominate. As a consequence of this capacity for initiating cracks within the contact cycle, the load-time configurations for which the instant of pop in just coincided with completion of the indentation cycle, defined by the condition $P = P_m^*$ and $t = T_m^*$, could be determined to relatively high accuracy. (Experimentally, these points were obtained by making series of indentations at preselected loads and systematically adjusting the pulse duration, decreasing or increasing T depending on whether pop in occurred without or within the load cycle.) Figure 4 shows data thus obtained for soda-lime glass and fused silica in air. A certain analogy may be noted between the plotting scheme in this figure and the lifetime plots used to characterize the fatigue strength of brittle materials¹¹

The data in Fig. 4 suggest a strong dependence of the initiation mechanics on molecular structure. We see that the threshold load in inert environments is substantially greater for soda-lime than for fused silica glass, ≈ 10 N compared to ≈ 5 N. On the other hand, soda-lime shows a relatively larger susceptibility to hydrolytic rate effects (as measured by the inverse slope of the lines through the data points), so that at loads below ≈ 1 N cracking generates more easily than in fused silica. The thresholds for quartz are much lower than for their glassy counterparts, below 0.5 N under even inert conditions; those indentations which did not produce radial cracks immediately did so within minutes on exposure to air. Similar observations on quartz have been reported by Nadeau.¹² It would appear that the main influence of structure lies in the magnitude, rather than the nature, of the initiation driving force that can be generated; the same qualitative effects are seen in all three materials studied, but with substantially different sensitivities to extraneous variables.

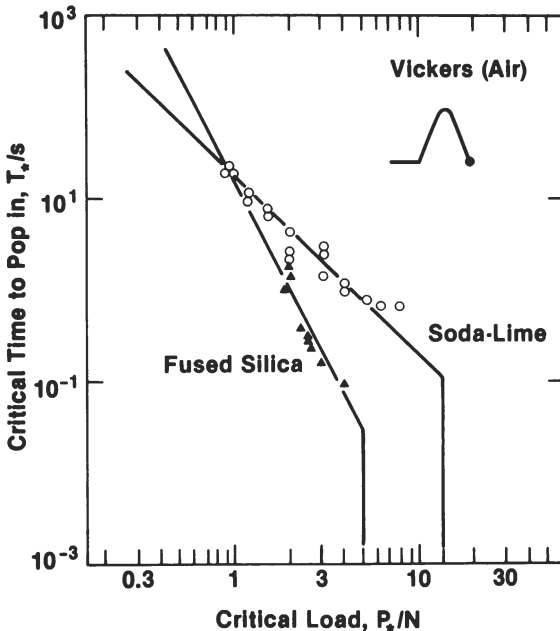


Figure 4. Plot of critical sinusoid load-time conditions to produce radial pop in at immediate unload point of contact cycle, for soda-lime and fused silica glasses in air. Vertical high-load cutoffs indicate spontaneous (time-independent) threshold limits in inert environments.

Microscopy of Indentations

Scanning electron microscopy provides some insight into the underlying mechanisms of radial crack initiation.¹⁻³ One of the most revealing procedures for observing the contact zone is to indent across a pre-existing hairline crack, and then to run this crack through the specimen to obtain a cross section view. Examples of Vickers indentations made in this way are shown in Fig. 5 for soda-lime and fused silica glass.

Such observations indicate that the non-recoverable component of the indentation deformation is a far from homogeneous process. Distinctive fine structure, on the micrometer scale, is apparent within the hardness impressions. This discrete detail may be interpreted in terms of an intermittent "faulting" mechanism, whereby the intense strains associated with the penetrating indenter are accommodated by local, catastrophic shear failures of the structure at the specimen surface.^{1,10,13,14} The periodicity of this "punching" mode is attributable to the need to build stresses back up to the theoretical strength of the glass after each fault is formed. The shear offsets associated with the fault traces on the free surfaces are measurably large, again on the order of micrometers,¹⁴ attesting to the catastrophic nature of the failure events. On etching in dilute hydrofluoric acid the fault traces show up much more clearly,² demonstrating that the slipped regions must have the character of high energy interfaces. It is clear from micrographs such as those in Fig. 5 that it is indeed these shear faults which provide the nuclei from which the radial cracks generate.

It is interesting at this point to examine the features of the fault patterns which differ in the materials studied. Some of these features may be distinguished in Fig. 5 for the two glass types. In soda-lime the faults propagate well into the subsurface region, ultimately intersecting with neighbors from other quadrants of the hardness impression. The high concentration of network modifier ions in this glass apparently provides more or less continuous paths of "easy slip" through the structure.^{10,15} In fused silica the absence of modifying elements precludes such cooperative slip modes, and the subsurface material accommodates the indentation volume by network densification.¹⁰ Accordingly, the stress intensifications associated with the surface faults are not so easily relieved in the fused silica (although in some favorable instances the constraints can be overcome by propagation into a cone crack configuration, Fig. 5), so the thresholds for radial initiation are somewhat lower than for soda-lime. On the other hand, the densification mode leaves the surrounding material in a relatively low state of residual strain, so the newly initiated radials do not propagate as far outward from the impression corners as do their counterparts in soda-lime glass.¹⁰

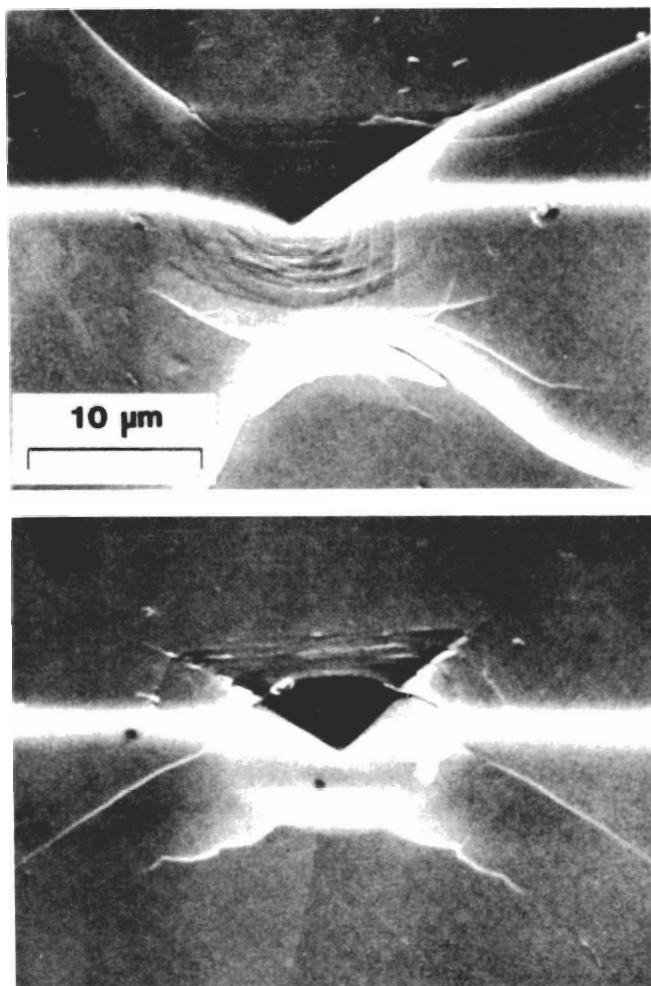


Figure 5. Scanning electron micrographs of Vickers indentations made at $P = 2$ N and $T = 10$ s in (a) soda-lime and (b) fused silica glasses, showing surface plus section views.

Similar fault markings are seen within surface indentations in quartz,^{16,17} with some indication that slip now occurs preferentially on certain crystallographic planes.¹⁶ It is conceivable that the additional constraints on the slip flexibility imposed by such crystallographic requirements could account for the ease with which cracks initiate in quartz, but our current understanding of the basic mechanisms of deformation in this material,¹² particularly in the subsurface deformation zone, is too obscure to allow for any more definitive a conclusion than this.

The question we now need to address is, do the observed shear fault patterns show any distinctive changes with contact duration? Our only attempts to answer this question thus far have been confined to observations using the optical microscope setup of Fig. 1. At the limits of resolution attainable with this setup one could just discern the incidence of individual shear events as lines of enhanced reflection within the square contact shadow of the Vickers pyramid. On reducing the contact duration the intensity of these reflections appeared to diminish. This trend correlated with an increasing "pincushion" distortion of the final impression; in soda-lime glass at $P = 1$ N, for instance, the ratio of "short" (edge center to opposing edge center) to "long" (corner to corner) dimensions (0.707 for ideal, square impression) dropped from 0.61 ± 0.02 at $T = 10$ s to 0.55 ± 0.02 at $T = 0.1$ s. The implication here is that the faults have less time to develop fully at the faster loading rates, indicating that the deformation process itself has an intrinsic kinetic element.

MODEL

The preceding observations lead us to a simple, two-step model for the crack initiation, depicted in Fig. 6.¹ The first step involves nucleation of the microcrack from which pop in ultimately ensues. The nucleation is expected to occur at points where the constraints on fault expansion are high, notably along the impression diagonals. Thus the major dimensions of the responsible defect configuration may remain effectively invariant during this stage of initiation; the process of stress intensification would then be more akin to flaw "sharpening" than to flaw "lengthening". The driving force for this first step comes from the shear component of the field, which reaches its maximum intensity at peak load but persists to a significant degree (as evidenced by the fact that the impression depth does not fully recover¹⁸) after removal of the indenter.

Step two involves growth of the newly formed microcrack to some critical instability point. The driving force now comes from the tensile component of the field which, as we have alluded, develops in the nucleation region only as the indenter is being

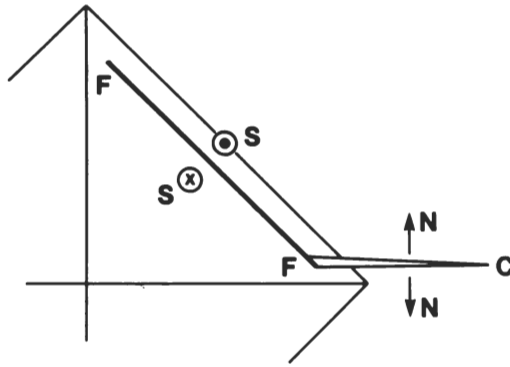


Figure 6. Schematic model of radial microcrack initiation FC from fault FF, in one quadrant of Vickers impression. Shear SS and normal NN stresses drive fault and crack respectively.

unloaded. Accordingly, this step should operate more effectively after than during the contact cycle. (This last assertion gains weight from the observation that reloading contact half-cycles cause any fully developed radial cracks to close up at the specimen surface.¹)

The fact that crack initiation occurs more easily at higher indentation loads (Fig. 2) could have its explanation in either of the two steps above. Generally, the effect of increasing the load is not to increase the intensity of the stress field (as governed by the hardness, which remains more or less invariant), but rather the spatial extent of this field.⁴ Thus in the nucleation stage we would expect the size of the embryo crack to increase in some proportion to the size of the critical shear fault. In the growth stage this same crack would be subject to smaller gradients of tensile stress in the field of larger impressions.⁶ At a sufficiently large indentation size the driving forces reach a level where both stages occur spontaneously, thereby defining the critical conditions for inert environments.

Insofar as rate effects are concerned, either step could exert a controlling influence. Here the paramount consideration is the role of water. This role has been explored in depth in the general deformation^{19,20} and fracture^{21,22} properties of amorphous and crystalline silicates. In terms of the specific model of Fig. 6, we expect the shear faults to provide preferred diffusion paths for atmospheric water; the interfaces, although in a basically compressive indentation zone, nevertheless represent planes of cohesive weakness, as evidenced by their susceptibility

to attack in etch solutions. Further, hydrolytic weakening of these interfaces ("decohesion") may then redistribute the active shear stresses, so as to build up the stress concentrations at the impression corners. Once nucleation has occurred, the water is free to enter the newly formed microcrack and promote slow growth.

This leaves us with the influence of contact duration to account for. Clearly, the data in Figs. 3 and 4 are qualitatively consistent with any load-dependent rate process. Decreasing T at given P effectively reduces the time available to drive the initiation during actual contact, thereby increasing the tendency to delayed pop in under the persistent action of the residual field. Our observation that the initiation does not reach completion within the initial, loading half-cycle now takes on a special significance. It suggests strongly that of the two stress components pertinent to our model, the shear driving the fault and the tension driving the microcrack (Fig. 6), it is the former which is the more crucial. We have implied that the normal stresses at potential initiation centers must remain highly compressive up to (and beyond) the peak contact configuration; and yet rate effects are evident even in square pulse experiments where the development of the residual tension is effectively instantaneous. Moreover, if initiation does not occur within the contact cycle the delay times can be inordinately large, orders of magnitude greater than the contact duration itself (Fig. 3), consistent with the assertion that the shear driving forces remain operative, but at diminished intensity, in the unloaded state. Finally, we may recall the tendency to less pronounced development of the shear fault configurations (as reflected in the increased pincushion distortion of the overall impressions) on going from relatively long ($T = 10$ s) to short ($T = 0.1$ s) contacts, corresponding to a shift from the spontaneous to the delayed pop-in regions in Fig. 3.

CONCLUSIONS

We have proposed a two-step, nucleation and growth, model of radial crack initiation beneath sharp indenters. The evidence on silicate structures presented in support of this model leads us to conclude that it is the micromechanics of "shear fault" evolution in the presence of interactive (moist) environments which hold the key to the strong rate dependence apparent in the threshold conditions. The nature of this evolution remains somewhat obscure. The faults clearly represent catastrophic failure events, operating at or close to the theoretical strength of the silicate structures, but do not fit in with the classical description of slip by dislocation motion and regeneration, or of fracture by a shearing mode; in the first instance the process occurs in both glassy and crystalline modifications of the SiO_2 structure, and in the second the existence of remnant interfacial

cohesive forces violates the requirement of stress-free boundaries. There is a need for closer investigation of these defect structures (e.g. by transmission electron microscopy) in different brittle materials, as well as of the crack nuclei that develop from these structures.

ACKNOWLEDGEMENTS

Funding for this study was provided by the U.S. Office of Naval Research, Metallurgy and Ceramics Program.

REFERENCES

1. B.R. Lawn, T.P. Dabbs and C.J. Fairbanks, J. Mater. Sci., in press.
2. T.P. Dabbs, C.J. Fairbanks and B.R. Lawn, in "Methods for Assessing the Structural Reliability of Brittle Materials," S.W. Freiman, ed., A.S.T.M. Special Technical Publication, in press.
3. B.R. Lawn, in "Strength of Glass," C.R. Kurkjian, ed., Plenum Press, in press.
4. B.R. Lawn and T.R. Wilshaw, J. Mater. Sci. 10:1049 (1975).
5. B.R. Lawn, A.G. Evans and D.B. Marshall, J. Amer. Ceram. Soc. 63:574 (1980).
6. B.R. Lawn and A.G. Evans, J. Mater. Sci. 12:2195 (1977).
7. K.E. Puttick, J. Phys. D.; Appl. Phys. 11:595 (1978).
8. T.P. Dabbs and B.R. Lawn, Phys. Chem. Glasses 23:93 (1982).
9. B.R. Lawn, D.B. Marshall and T.P. Dabbs, in "Strength of Glass," C.R. Kurkjian, ed., Plenum Press, in press.
10. A. Arora, D.B. Marshall, B.R. Lawn and M.V. Swain, J. Non-Cryst. Solids 31:915 (1979).
11. R.F. Cook and B.R. Lawn, in "Methods for Assessing the Structural Reliability of Brittle Materials," S.W. Freiman, ed., A.S.T.M. Special Technical Publication, in press.
12. J.S. Nadeau, J. Amer. Ceram. Soc. 53:568 (1970).
13. J.T. Hagan and M.V. Swain, J. Phys. D.; Appl. Phys. 11:2091 (1978).

14. J.T. Hagan, J. Mater. Sci. 15:1417 (1980).
15. F.M. Ernsberger, J. Non-Cryst. Solids 25:293 (1977).
16. W.F. Brace, J. Geology 71:581 (1963).
17. M.V. Swain, Ph.D. Thesis, University of New South Wales, Australia, 1973.
18. B.R. Lawn and V.R. Howes, J. Mater. Sci. 16:2475 (1981).
19. D.T. Griggs and J.D. Blacic, Science 147:292 (1965).
20. S.P. Gunasekera and D.G. Holloway, Phys. Chem. Glasses 14:45 (1973).
21. S.M. Wiederhorn and L.H. Bolz, J. Amer. Ceram. Soc. 53:543 (1970).
22. C.H. Sholz and R.J. Martin, J. Amer. Ceram. Soc. 54:474 (1971).